

Suitability of $^{210}\text{Pb}_{\text{ex}}$, ^{137}Cs and $^{239+240}\text{Pu}$ as soil erosion tracers in western Kenya

Sophia M. Dowell^{a,b}, Olivier S. Humphrey^a, Charles J.B. Gowing^a, Thomas S. Barlow^a, Simon R. Chenery^a, Job Isaboke^c, William H. Blake^b, Odipo Osano^c, Michael J. Watts^{a,*}

^a Inorganic Geochemistry, Centre for Environmental Geochemistry, British Geological Survey, Nottingham, NG12 5GG, UK

^b School of Geography, Earth and Environmental Sciences, University of Plymouth, Plymouth, Devon, PL4 8AA, UK

^c School of Environmental Sciences, University of Eldoret, Eldoret, Kenya

ARTICLE INFO

Keywords:

$^{239+240}\text{Pu}$
 $^{210}\text{Pb}_{\text{ex}}$
 ^{137}Cs
 Fallout radionuclides
 Soil erosion
 Kenya

ABSTRACT

Land degradation resulting from soil erosion is a global concern, with the greatest risk in developing countries where food and land resources can be limited. The use of fallout radionuclides (FRNs) is a proven method for determining short and medium-term rates of soil erosion, to help improve our understanding of soil erosion processes. There has been limited use of these methods in tropical Africa due to the analytical challenges associated with ^{137}Cs , where inventories are an order of magnitude lower than in the Europe. This research aimed to demonstrate the usability of $^{239+240}\text{Pu}$ as a soil erosion tracer in western Kenya compared to conventional isotopes $^{210}\text{Pb}_{\text{ex}}$ and ^{137}Cs through the determination of FRN depth profiles at reference sites. Across six reference sites $^{239+240}\text{Pu}$ showed the greatest potential, with the lowest coefficient of variation and the greatest peak-to-detection limit ratio of 640 compared to 5 and 1 for $^{210}\text{Pb}_{\text{ex}}$ and ^{137}Cs respectively. Additionally, $^{239+240}\text{Pu}$ was the only radionuclide to meet the 'allowable error' threshold, demonstrating applicability to large scale studies in Western Kenya where the selection of suitable reference sites presents a significant challenge. The depth profile of $^{239+240}\text{Pu}$ followed a polynomial function, with the maximum areal activities found between depths 3 and 12 cm, where thereafter areal activities decreased exponentially. As a result, $^{239+240}\text{Pu}$ is presented as a robust tracer to evaluate soil erosion patterns and amounts in western Kenya, providing a powerful tool to inform and validate mitigation strategies with improved understanding of land degradation.

1. Introduction

Accelerated soil erosion is a growing global concern, presenting the largest worldwide threat to land degradation and soil erosion may be intensified, particularly in developing countries resulting in a significant obstacle for the intensification of agriculture (Alewell et al., 2014; Deepak Lal, 2000; Lal, 2001; Lorenz et al., 2019; Pimentel, 2006). Inadequate land management techniques and vegetation clearance are major drivers of soil erosion, and with changes in precipitation as a result of climate change, soil erosion will be intensified to unsustainable levels (Borrelli et al., 2020; Negese, 2021). Quantitative data describing the amounts and patterns of soil erosion and sedimentation can be used to inform sustainable soil conservation practices. This data can also aid in the validation of predictive models for an improved understanding of factors influencing the acceleration of erosion processes (Boardman, 2006; Joint FAO/IAEA Division of Nuclear Techniques in Food and

Agriculture, Soil and Water Management and Crop Nutrition Section, 2014; Loba et al., 2022).

In Africa, traditional approaches such as erosion plots, surveying, and the use of aerial photography have been employed for decades to evaluate erosion process, however, they have several disadvantages, including poor representativeness and spatial resolution (Elwell, 1978; Whitlow, 1988). More recently, tracer methods using fallout radionuclides (FRNs) have been employed to determine long term rates of soil erosion over a period of >80 years. Without the need for costly long-term monitoring approaches, these strategies provide an alternative for quantifying soil erosion. In contrast to conventional methods, FRNs can quantify both erosion and deposition rates within a single sampling campaign, with the resulting erosional rates being representative of all redistribution processes (Alewell et al., 2017; Hou, 2019; Loba et al., 2022; Meusburger et al., 2018; Schimmack et al., 2004).

A critical requirement associated with the use of FRN to determine

* Corresponding author.

E-mail address: mwatts@bgs.ac.uk (M.J. Watts).

<https://doi.org/10.1016/j.jenvrad.2023.107327>

Received 4 August 2023; Received in revised form 27 September 2023; Accepted 28 October 2023

Available online 9 November 2023

0265-931X/Crown Copyright © 2023 Published by Elsevier Ltd.

This is an open access article under the CC BY license

(<http://creativecommons.org/licenses/by/4.0/>).

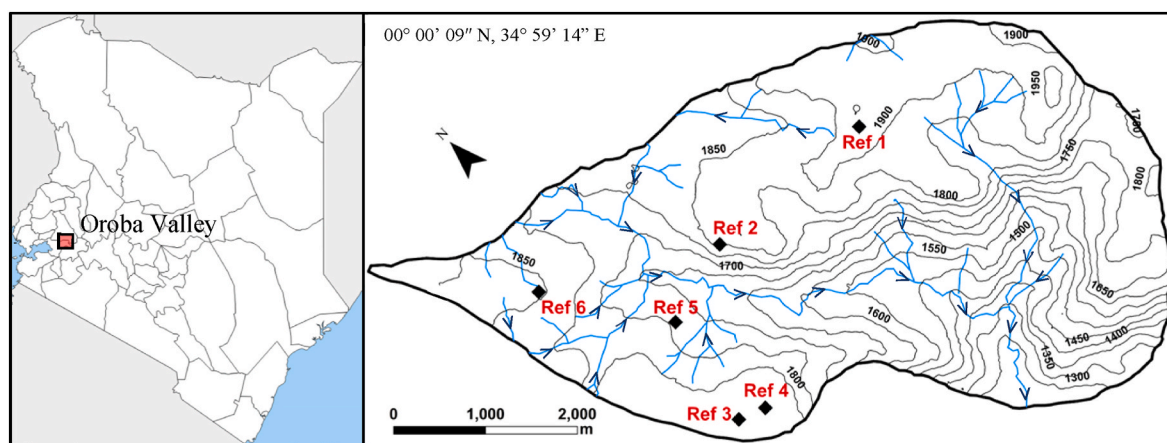


Fig. 1. Sample location of reference soil cores within the Oroba river catchment, Nandi County, Kenya. Map created using the GADM database.

rates of soil erosion is the selection of suitable reference sites. A typical reference site will be a flat, well vegetated, and unploughed area, to limit any possible soil redistribution at that site. In addition, as the FRN inventory at the reference site is assumed to represent the baseline fallout, it is important that the fallout of the FRN was spatially uniform across the study site (Joint FAO/IAEA Division of Nuclear Techniques in Food and Agriculture, Soil and Water Management and Crop Nutrition Section, 2014). The most frequently used FRNs for the assessment of long-term erosion studies were unsupported lead-210 ($^{210}\text{Pb}_{\text{ex}}$) and caesium-137 (^{137}Cs). However, plutonium ($^{239+240}\text{Pu}$) has gained recognition due to its long-term availability and advancements in detection using ICP-MS technology (Alewell et al., 2014; Dowell et al., 2023a; Gerd R. Ruecker et al., 2008; Meusburger et al., 2018).

Within tropical Africa, the limited application of these methods is likely due to the analytical challenges associated with ^{137}Cs analysis, as its inventories are an order of magnitude lower than in Europe. In Eastern Africa, studies utilising ^{137}Cs as a tracer for soil erosion have been reported in Uganda, Kenya, and Ethiopia with values ranging between 200 and 2064 Bq m^{-2} at reference sites (DeGraffenried and Shepherd, 2009; Denboba AM, 2005; Gerd R. Ruecker et al., 2008). In Kenya, DeGraffenried and Shepherd, 2009, reported that ^{137}Cs inventory was below the detection limit of 30 Bq m^{-2} , highlighting the challenges associated with the determination of ^{137}Cs activity in the tropics. Wilken et al. (2020), reported the application of $^{239+240}\text{Pu}$ as a soil erosion tracer with study sites in Democratic Republic of the Congo Uganda and Rwanda in three forest reference sites with mean $^{239+240}\text{Pu}$ inventories between 33 and 48 Bq m^{-2} . The aim of this paper was to demonstrate the utility of $^{239+240}\text{Pu}$ as a soil erosion tracer in western Kenya compared to $^{210}\text{Pb}_{\text{ex}}$ and ^{137}Cs with the objectives of 1) determining depth profiles of FRNs at six reference sites, 2) identifying the robustness of each FRN by calculating the coefficient of variations and 3) assessing the improved applicability of $^{239+240}\text{Pu}$ to large scale studies compared to other FRNs.

2. Materials and methods

2.1. Study area and soil sampling design

The study area was located within the Rift Valley, Nandi County, Kenya. The valley banks onto the Oroba river which drains into the Winam gulf of Lake Victoria. This valley was indicated to be at increased risk of erosion by Humphrey et al. (2022), with continuous land clearance over the past 80 years. According to the requirements of IAEA's 2014 guidelines, six suitable reference sites were identified (Fig. 1) (Joint FAO/IAEA Division of Nuclear Techniques in Food and Agriculture, Soil and Water Management and Crop Nutrition Section, 2014).

At each reference site a 30 cm core with a 5 cm diameter was

excavated and split into 10 sections to determine the inventories of $^{210}\text{Pb}_{\text{ex}}$, ^{137}Cs and $^{239+240}\text{Pu}$. The bulk density was determined following sample drying at 30 °C for 24 h or until the soils were fully dry, and then the sample was sieved to <2 mm before reweighing to determine the soil density (U.S. EPA, 1996; FAO, 2020). The average soil density calculated was 1.32 and values ranged from 0.82 to 1.66 g cm^{-3} , with density increasing down the core. The depth profile data for $^{239+240}\text{Pu}$ at site 3 was previously published by Dowell et al. (2023b).

2.2. Sample preparation and analysis

2.2.1. Gamma spectroscopy – $^{210}\text{Pb}_{\text{ex}}$ and ^{137}Cs

Prior to analysis, the sieved soils (<2 mm) were placed into 147 mL polystyrene pots (base diameter 60 mm) with no headspace and sealed for 21 days to achieve equilibrium between ^{226}Ra and ^{222}Rn . After this time measurements of ^{137}Cs , ^{210}Pb and ^{226}Ra (via analysis of ^{214}Pb) activities were determined using a high resolution HPGe gamma detector at the British Geological Survey, Nottingham (Canberra Mirion, BE3825 with 71 mm active diameter and a carbon epoxy composite end cap, operated at a bias of +4 kV). Samples were counted between 24 and 48 h (until the measured activity exceeded the Minimal Detectable Activity (MDA)). The measured spectrum was fitted using Genie 2000 software (Mirion technologies Inc, Atlanta, USA) and corrected for spectral background. Efficiency corrections were performed using Lab-SOCS calibration software (Mirion technologies Inc, Atlanta, USA) and spectral peaks were fitted against a library containing natural nuclide emission line energies from the ^{238}U , ^{235}U and ^{232}Th series. The Currie equation was used to calculate MDAs. Instrument QA was performed by analysis of ^{241}Am , ^{137}Cs and ^{60}Co spot sources. The unsupported ^{210}Pb ($^{210}\text{Pb}_{\text{ex}}$) activity was then calculated by the subtraction of supported ^{210}Pb (^{214}Pb equivalent) activity from the total ^{210}Pb activity in the sample.

2.2.2. ICP-MS/MS – $^{239+240}\text{Pu}$

The full analytical procedure for ICP-MS/MS analysis is outlined in Dowell et al. (2023b). Prior to analysis the soil samples were milled, and 50 g was weighed into a glass beaker. This sample was then ashed overnight. The ashed samples were placed into a PTFE beaker with a 50 μg of a ^{242}Pu spike to be leached using 100 ml concentrated HNO_3 . The soil solution was then heated on a hotplate at 70 °C for 24 h, and then centrifuged. The supernatant was filtered through a 0.45 μm hydrophilic PTFE filter and collected. To adjust the Pu oxidation state to IV for the separation, 0.02 g NaNO_2 per 1 ml of solution was added. The Pu in the solution was then separated from interfering isotopes using a TEVA column separation. Within each dissolution process two silica sand column blanks (20 g) along with CRM sample IAEA 384 (0.5 g) were analysed to ensure validity of the analytical procedure and to determine

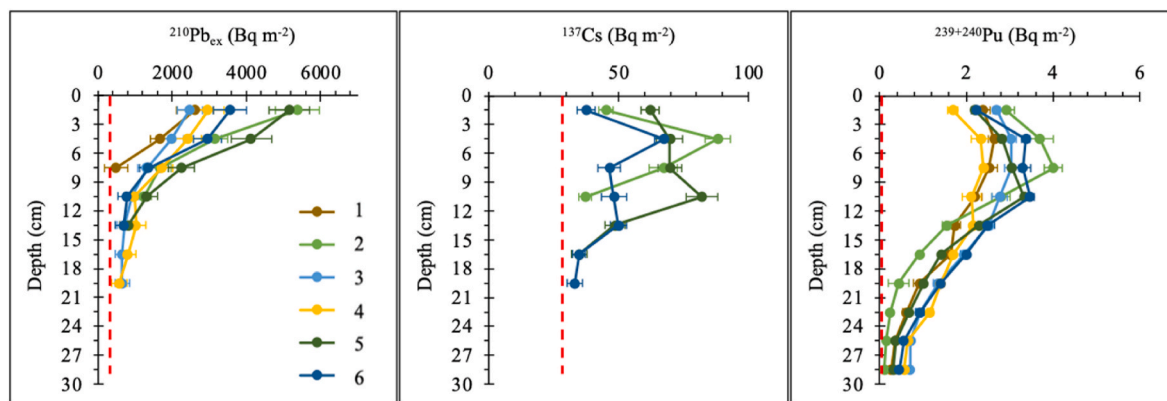


Fig. 2. Areal activity depth distribution patterns at the six reference sites for $^{210}\text{Pb}_{\text{ex}}$, ^{137}Cs and $^{239+240}\text{Pu}$ with detection limits (red dashed line). (For interpretation of the references to colour in this figure legend, the reader is referred to the Web version of this article.)

Table 1

Limits of detection and depth distribution patterns for $^{210}\text{Pb}_{\text{ex}}$, ^{137}Cs (gamma spectrometry) and $^{239} + ^{240}\text{Pu}$ (ICP-MS/MS using O_2 reaction gas).

Isotope	Detection Limit (Bq m^{-2})	Max peak/ Detection limit	Areal activity in top 3 cm (%)	Areal activity in top 12 cm (%)
$^{210}\text{Pb}_{\text{ex}}$	498	5	39	90
^{137}Cs	31	1	16	80
$^{239+240}\text{Pu}$	6×10^{-3}	640	13	63

the detection limits. The decontamination factor achieved for U isotopes after column separation was 200.

An ICP-MS/MS (Agilent 8900, Agilent Technologies, Japan) was used for the measurement of Pu isotopes in the soil samples with O_2 gas in the collision-reaction cell. The sample was introduced using an Agilent IaS micro-autosampler and a Cetac Aridus II desolvating nebuliser (Teledyne CETAC Technologies, Omaha, USA). The instrument was calibrated for sensitivity using a ^{238}U standard as no certified Pu standard was available (Dowell et al., 2023b). Average $^{239+240}\text{Pu}$ dioxide counts for the samples were 604 counts per second with an average background of 3 counts per second. A concentration of 100 pg kg^{-1} is equivalent to 350 counts per second of $^{239+240}\text{Pu}$ dioxide. The mean spike recoveries of the samples was 79%. The isotope ratio of $^{240}\text{Pu}/^{239}\text{Pu}$ was also measured alongside the $^{239+240}\text{Pu}$ activities for each sample where all sampling sites had a ratio of 0.18 ± 0.02 which agrees with the stratospheric global fallout ratio of 0.18 ± 0.014 (Kelley et al., 1999). Further details on the analytical methods performance have been published (open access) by Dowell et al. (2023b).

Table 2

Total inventory of $^{210}\text{Pb}_{\text{ex}}$, ^{137}Cs and $^{239+240}\text{Pu}$ ($\pm 2\sigma$) and validity of reference site measurements to determine soil redistribution rates in the Oroba valley, Nandi County, Kenya.

Site	$^{210}\text{Pb}_{\text{ex}}$		^{137}Cs		$^{239+240}\text{Pu}$	
	Maximum depth (cm)	inventory (Bq m^{-2})	Maximum depth (cm)	inventory (Bq m^{-2})	Maximum depth (cm)	inventory (Bq m^{-2})
1	9	2385 ± 1178	–	–	30	15 ± 0.3
2	12	5721 ± 627	12	119 ± 8	30	17 ± 0.4
3	21	4360 ± 884	–	–	30	20 ± 0.5
4	21	5246 ± 817	–	–	30	16 ± 0.3
5	15	6840 ± 737	18	184 ± 11	30	18 ± 0.4
6	15	4681 ± 768	21	159 ± 10	30	20 ± 0.8
Mean	4872 ± 2996		154 ± 66		18 ± 4.1	
CV (%)	30.7		21.2		11.1	
AE (%)	25.3		28.8		9.2	

3. Results and discussion

The $^{210}\text{Pb}_{\text{ex}}$ areal activities for the six reference sites decreased exponentially with depth following a polynomial distribution, where the maximum areal activity was found within the first 3 cm of the soil core (Fig. 2). This agrees with similar findings in the literature and is due to continual deposition of $^{210}\text{Pb}_{\text{ex}}$ into the soil as a result of rain-out (Meusburger et al., 2018). Although samples down to a depth of 30 cm were counted, it was not possible to detect $^{210}\text{Pb}_{\text{ex}}$ above the MDA beneath a depth of 21 cm. The depth distribution of both ^{137}Cs and $^{239+240}\text{Pu}$ at the reference sites follow a polynomial function with the maximum areal activities found between depths of 3–12 cm, where thereafter areal activities decreased exponentially. This has been shown to be a common depth distribution pattern and can be explained by the downward migration of isotopes in the time since the major bomb fallout events (Alewell et al., 2014, 2017; Lal et al., 2013; Zhang et al., 2019).

Only three of the reference sites had measurable ^{137}Cs above the MDA and quantification was only possible to a maximum depth of 21 cm. The measurement of both $^{210}\text{Pb}_{\text{ex}}$ and ^{137}Cs is severely limited by the achievable MDAs using gamma spectrometry, which although requiring a much simpler sample preparation procedure, has much lower throughput than the ICP-MS/MS methodology due to long counting times, limiting applicability of the method (Table 1). On the other hand, $^{239+240}\text{Pu}$ which was determined using ICP-MS/MS with O_2 reaction gas was quantified in all samples down to the total depth of 30 cm and with much greater peak to detection limit ratios.

Using the test proposed by Sutherland, (1996) the validity and accuracy of the reference values was verified by calculating the allowable error (AE) at the 90% confidence level where n is the number of samples and t is the student's t-value for an $\alpha = 0.10$ (90% confidence level (Equation (1))). The coefficients of variation (CV) for $^{210}\text{Pb}_{\text{ex}}$, ^{137}Cs and

$^{239+240}\text{Pu}$ were 31%, 21% and 11%, respectively (Table 2). Considering the number of samples, the AE was calculated as 25% for $^{210}\text{Pb}_{\text{ex}}$, 29% for ^{137}Cs and 9% for $^{239+240}\text{Pu}$. Only Pu meets the requirement of having an AE $\leq 10\%$ while the number of reference sites for ^{210}Pb and ^{137}Cs would need to be increased until the AE criteria was met (Mabit et al., 2012; Meusburger et al., 2018; Sutherland, 1996).

$$n' = \left[\frac{t_{(\alpha, n-1)} CV}{AE} \right]^2 \quad (1)$$

Equation 1 – Equation for the calculation of allowable error (AE) (Sutherland, 1996).

The mean activity concentrations for ^{137}Cs was below previously reported values for non-eroded sites in Kenya reported by DeGraffenried and Shepherd, 2009 of 4.15 Bq kg^{-1} (Table S1). This is likely as a result of ^{137}Cs 's short half-life and the 14 years between the studies. In Eastern Africa, studies utilising ^{137}Cs as a tracer for soil erosion reported inventories have been reported between 200 and 2064 Bq m^{-2} at reference sites in Uganda and Ethiopia (Denboba, 2005; Gerd R. Ruecker et al., 2008; DeGraffenried and Shepherd, 2009). The mean inventory of the six reference sites for $^{239+240}\text{Pu}$ of 18 Bq m^{-2} is consistent with the regional fallout estimations by Hardy et al., 1973; Kelley et al., 1999 of 19.2 Bq m^{-2} , further supporting the validity of the reference site measurements. The results presented support the hypothesis that $^{239+240}\text{Pu}$ has the potential to be used as the preferred FRN tracer in western Kenya, with low achievable allowable error across the reference sites, allowing for greater applicability to study sites where the selection of appropriate reference sites is a challenge.

4. Conclusion

Here we assessed the suitability of $^{239+240}\text{Pu}$ as a soil erosion tracer in western Kenya compared to traditionally used FRNs $^{210}\text{Pb}_{\text{ex}}$ and ^{137}Cs . Reference sites to evaluate the potential of FRN were selected according to the guidelines set out by IAEA 2014; Joint FAO/IAEA Division of Nuclear Techniques in Food and Agriculture, Soil and Water Management and Crop Nutrition Section, 2014). Depth profiles of $^{210}\text{Pb}_{\text{ex}}$, ^{137}Cs , and $^{239+240}\text{Pu}$ were determined to establish the suitability of each radionuclide for the determination of soil erosion rates. Of the three elements, $^{239+240}\text{Pu}$ was the only one that met the requirements to be used as a reference set out by Sutherland. (1996), with an 'allowable error' of $\leq 10\%$ across the six reference sites. This is likely a result of the advancements in analysis using ICP-MS/MS, where a much greater peak-to-detection limit ratio was achievable for $^{239+240}\text{Pu}$ compared to $^{210}\text{Pb}_{\text{ex}}$ and ^{137}Cs , allowing for greater precision and determination to greater depth. The low coefficient of variation and allowable error for $^{239+240}\text{Pu}$ across the reference sites indicates the applicability of Pu as a robust tracer of soil erosion in western Kenya with applicable to large scale studies compared to other FRN tracers. The need for fewer reference sites, as a result of the low allowable error, lends well to study sites where the selection of appropriate reference sites is a challenge. The use of $^{239+240}\text{Pu}$ as a robust soil erosion tracer will play a vital role in the determination of soil degradation amounts and patterns, providing a powerful tool to improve our understanding of the effectiveness of mitigation strategies.

Declaration of competing interest

There are no conflicts to declare.

Data availability

Data will be made available on request.

Acknowledgements

This work is published with the permission of the Executive Director, British Geological Survey. This work has originated from research conducted with the financial support of the following funders: BGS-NERC grant NE/R000069/1 entitled 'Geoscience for Sustainable Futures' and BGS Centre for Environmental Geochemistry programmes, the NERC National Capability International Geoscience programme entitled 'Geoscience to tackle global environmental challenges' (NE/X006255/1). Additionally financial support from The Royal Society international collaboration awards 2019 grant ICA/R1/191077 entitled 'Dynamics of environmental geochemistry and health in a lake wide basin', Natural Environment Research Councils ARIES Doctoral Training Partnership (grant number NE/S007334/1) and the British Geological Survey University Funding Initiative (GA/19S/017) was provided, alongside support provided from the British Academy Early Career Researchers Writing Skills Workshop (WW21100104).

Appendix A. Supplementary data

Supplementary data to this article can be found online at <https://doi.org/10.1016/j.jenvrad.2023.107327>.

References

- Alewell, C., Meusburger, K., Juretzko, G., Mabit, L., Ketterer, M.E., 2014. Suitability of $^{239+240}\text{Pu}$ and ^{137}Cs as tracers for soil erosion assessment in mountain grasslands. *Chemosphere* 103, 274–280. <https://doi.org/10.1016/j.chemosphere.2013.12.016>.
- Alewell, C., Pitois, A., Meusburger, K., Ketterer, M., Mabit, L., 2017. $^{239+240}\text{Pu}$ from "contaminant" to soil erosion tracer: where do we stand? *Earth Sci. Rev.* 172, 107–123. <https://doi.org/10.1016/j.jearthsci.2017.07.009>.
- Boardman, J., 2006. Soil erosion science: reflections on the limitations of current approaches. In: *Catena (Amst)*, vol. 68, pp. 73–86. <https://doi.org/10.1016/j.catena.2006.03.007>.
- Borrelli, P., Robinson, D.A., Panagos, P., Lugato, E., Yang, J.E., Alewell, C., Wuepper, D., Montanarella, L., Ballabio, C., 2020. Land use and climate change impacts on global soil erosion by water (2015–2070). *Proc. Natl. Acad. Sci. USA* 117, 21994–22001. <https://doi.org/10.1073/pnas.2001403117>.
- DeGraffenried, J.B., Shepherd, K.D., 2009. Rapid erosion modeling in a Western Kenya watershed using visible near infrared reflectance, classification tree analysis and ^{137}Cs . *Geoderma* 154, 93–100. <https://doi.org/10.1016/j.geoderma.2009.10.001>.
- Denboba, A.M., 2005. *Forest Conversion-Soil Degradation-Farmers Perception Nexus: Implications for Sustainable Land Use in the Southwest of Ethiopia*, vol. 26. Cuvillier Verlag.
- Dowell, S.M., Humphrey, O.S., Blake, W.H., Osano, O., Chenery, S., Watts, M.J., 2023a. Ultra-trace analysis of fallout plutonium isotopes in soil: emerging trends and future perspectives. *Chemistry Africa*. <https://doi.org/10.1007/s42250-023-00659-7>.
- Dowell, S.M., Barlow, T.S., Chenery, S.R., Humphrey, O.S., Isaboke, J., Blake, W.H., Osano, O., Watts, M.J., 2023b. Optimisation of plutonium separations using TEVA cartridges and ICP-MS/MS analysis for applicability to large-scale studies in tropical soils. *Anal. Methods*. <https://doi.org/10.1039/D3AY01030A>.
- Elwell, H.A., 1978. Modelling soil losses in southern Africa. In: *Journal of Agricultural Engineering Research*, vol. 23, pp. 117–127. [https://doi.org/10.1016/0021-8634\(78\)90043-4](https://doi.org/10.1016/0021-8634(78)90043-4).
- FAO, 2020. *Soil Testing Methods – Global Soil Doctors Programme - A Farmer-To-Farmer Training*. <https://doi.org/10.4060/ca2796en>. Programme. Rome.
- Hardy, E.P., Krey, P.W., Volchok, H.L., 1973. *Global Inventory and Distribution of Fallout Plutonium*[1]. <https://doi.org/10.1038/241444a0>. *Nature*.
- Hou, X., 2019. Radioanalysis of ultra-low level radionuclides for environmental tracer studies and decommissioning of nuclear facilities. *J. Radioanal. Nucl. Chem.* 322, 1217–1245. <https://doi.org/10.1007/s10967-019-06908-9>.
- Humphrey, O.S., Osano, O., Aura, C.M., Marriott, A.L., Dowell, S.M., Blake, W.H., Watts, M.J., 2022. Evaluating spatio-temporal soil erosion dynamics in the Winam Gulf catchment, Kenya for enhanced decision making in the land-lake interface. *Sci. Total Environ.* 815, 151975. <https://doi.org/10.1016/j.scitotenv.2021.151975>.
- Joint FAO/IAEA Division of Nuclear Techniques in Food and Agriculture, Soil and Water Management and Crop Nutrition Section, Vienna (Austria), 2014. In: *Guidelines for Using Fallout Radionuclides to Assess Erosion and Effectiveness of Soil Conservation Strategies (IAEA-TECDOC-1741)*. International Atomic Energy Agency (IAEA).
- Kelley, J.M., Bond, L.A., Beasley, T.M., 1999. Global distribution of Pu isotopes and ^{237}Np . *Sci. Total Environ.* 237–238, 483–500. [https://doi.org/10.1016/S0048-9697\(99\)00160-6](https://doi.org/10.1016/S0048-9697(99)00160-6).
- Lal, Deepak, 2000. *The Poverty of "Development Economics"*, second ed. The MIT Press, Massachusetts.
- Lal, R., 2001. Soil degradation by erosion. *Land Degrad. Dev.* 12, 519–539. <https://doi.org/10.1002/ldr.472>.

- Lal, R., Tims, S.G., Fifield, L.K., Wasson, R.J., Howe, D., 2013. Applicability of ²³⁹Pu as a tracer for soil erosion in the wet-dry tropics of northern Australia. *Nucl. Instrum. Methods Phys. Res. B* 294, 577–583. <https://doi.org/10.1016/j.nimb.2012.07.041>.
- Loba, A., Waroszewski, J., Sykula, M., Kabala, C., Egli, M., 2022. Meteoric ¹⁰Be, ¹³⁷Cs and ²³⁹⁺²⁴⁰Pu as tracers of long- and medium-term soil erosion - a review, 2022 *Minerals* 12, 359. <https://doi.org/10.3390/MIN12030359>, 359–12.
- Lorenz, K., Lal, R., Ehlers, K., 2019. Soil organic carbon stock as an indicator for monitoring land and soil degradation in relation to United Nations' Sustainable Development Goals. *Land Degrad. Dev.* 30, 824–838. <https://doi.org/10.1002/ldr.3270>.
- Mabit, L., Chhem-Kieth, S., Toloza, A., Vanwalleghem, T., Bernard, C., Amate, J.I., Gómez, J.A., 2012. Radioisotopic and physicochemical background indicators to assess soil degradation affecting olive orchards in southern Spain. *Agric. Ecosyst. Environ.* 159, 70–80. <https://doi.org/10.1016/j.agee.2012.06.014>.
- Meusburger, K., Porto, P., Mabit, L., La Spada, C., Arata, L., Alewell, C., 2018. Excess Lead-210 and Plutonium-239+240: two suitable radiogenic soil erosion tracers for mountain grassland sites. *Environ. Res.* 160, 195–202. <https://doi.org/10.1016/J.ENVIRES.2017.09.020>.
- Negese, A., 2021. Impacts of land use and land cover change on soil erosion and hydrological responses in Ethiopia. *Appl Environ Soil Sci* 2021 1–10. <https://doi.org/10.1155/2021/6669438>.
- Pimentel, D., 2006. Soil erosion: a food and environmental threat. *Environ. Dev. Sustain.* 8, 119–137. <https://doi.org/10.1007/s10668-005-1262-8>.
- Ruecker, Gerd R., Soojin, J. Park, Almut C, Brunner, Paul L, G. Vlek, 2008. Assessment of soil redistribution on two contrasting hillslopes in Uganda using caesium-137 modelling. *Erdkunde* 62, 259–272. <https://www.jstor.org/stable/25648129>.
- Schimmack, W., Auerswald, K., Bunzl, K., 2004. Estimation of soil erosion and deposition rates at an agricultural site in Bavaria, Germany, as derived from fallout radiocesium and plutonium as tracers. *Naturwissenschaften* 2001 89 (1 89), 43–46. <https://doi.org/10.1007/S00114-001-0281-Z>.
- Sutherland, R.A., 1996. Caesium-137 soil sampling and inventory variability in reference locations: a literature survey. *Hydrol. Process.* 10, 43–53. [https://doi.org/10.1002/\(SICI\)1099-1085\(199601\)10:1<43::AID-HYP298>3.0.CO;2-X](https://doi.org/10.1002/(SICI)1099-1085(199601)10:1<43::AID-HYP298>3.0.CO;2-X).
- U.S. EPA, 1996. *Method 3050B: Acid Digestion of Sediments, Sludges, and Soils,* Revision 2. Washington, DC.
- Whitlow, R., 1988. *Land Degradation in Zimbabwe: a Geographical Study.* UZ/ Department of Natural Resources, Harare.
- Wilken, F., Fiener, P., Ketterer, M., Meusburger, K., Muhindo, D.I., Van Oost, K., Doetterl, S., 2020. Assessing soil erosion of forest and cropland sites in wet tropical Africa using ²³⁹⁺²⁴⁰Pu fallout radionuclides, 2020 *Soil Discussions* 1–22. <https://doi.org/10.5194/soil-2020-95>.
- Zhang, W., Xing, S., Hou, X., 2019. Evaluation of soil erosion and ecological rehabilitation in Loess Plateau region in Northwest China using plutonium isotopes. *Soil Tillage Res.* 191, 162–170. <https://doi.org/10.1016/J.STILL.2019.04.004>.